

Line Profile Based Segmentation Algorithm for Touching Corn Kernels

Ali Mahdi and Jun Qin

Department of Electrical and Computer Engineering

Southern Illinois University Carbondale

Abstract: Image segmentation of touching objects plays a key role in providing accurate classification for computer vision technologies. A new line profile based imaging segmentation algorithm has been developed to provide a robust and accurate segmentation of a group of touching corns. The performance of the line profile based algorithm has been compared to a watershed based imaging segmentation algorithm. Both algorithms are tested on three different patterns of images, which are isolated corns, single-lines, and random distributed formations. The experimental results show that the algorithm can segment a large number of touching corn kernels efficiently and accurately.

Keywords: Touching corn kernels, segmentation, line profile, concavity, watershed

1. Introduction

United States Department of Agriculture (USDA) ¹ states that corn is the most produced crop with 984.37 million metric tons in the United States in 2014. Today, the Federal Grain Inspection Service (FGIS), Packers and stockyards Administration (GIPSA) of the United States Department of Agriculture (USDA) ² control and manage the grain grading standards. Various informal grading methods are currently being used in the market by smaller facilities to avoid the complexity involved in performing the official test. The unofficial grading results may vary between individual operators due to human subjectivity and less training. Due to the expectations for food production of high quality and safety standards, computer recognition was introduced to improve grading results ³.

Previous studies have shown that computer vision could be a viable method for analyzing grain ⁴ ¹². Paulsen et al ^{4, 13} developed a computer recognition prototype to classify the corn based on size and crown shape. Steenhoek et al ⁵ devised a machine learning system to evaluate and classify corn kernels based on damage type. Chen et al ⁶ combined computer vision and pattern classification to identify and five varieties of corn based on geometric, shape, and colour

features. Valiente-Gonzalez et al ¹⁴ designed a computer vision system for automated evaluation of the quality of corn lot. In many previous studies, the focus was on studying images of separated grains. But today, many image segmentation algorithms are introduced to separate touching grains.

Visen et al ¹⁵ devised an algorithm to separate the touching grain kernels. The algorithm consists of two steps. The first step identifies each object as either an isolate kernel or a cluster of touching kernels based on ellipse fitting. The second step separates the touching objects within a cluster based on detecting the curvature of the boundary. Wang and Paliwal ¹⁶ developed a morphological method based on watershed transform of the distance transform of the image to separate rice kernels. Over segments of the same object are rejoined to reduce the over segmentation by reconstructing the internal markers. Faessel and Courtois ¹⁷ devised an approach to separate rice kernels using the gap filling technique. The skeleton of the background of the image is determined resulting open lines. These lines are prolonged and the end points of the lines are connected if the distance between them is smaller than a specific threshold. Zhong et al ¹⁸ developed a novel segmentation algorithm based on watershed and concavities to separate slender particles like rice kernels. Using the concavity features, the over segmented objects are merged back to their original object. A split path is determined between the un-segmented objects. A supplementary criterion is applied to decide if the split line is accepted or not. Yan et al ¹⁹ devised a segmentation algorithm based on contour segments and ellipse fitting to segment six types of Korean grains. The contour of each object is divided into segments, and concave points are located on the segments. Two tools are used to decide if the contour segment is merged to the new image. These tools are distance measurement, and error deviation measurement. Qin et al ³ modified the watershed method to provide accurate segmentation of the corn. Distance transformed image is first processed using the extended maxima transform, then the binary image is determined, and then watershed is applied. Finally, touching corn kernels are separated into segments.

In this study, a computer vision system has been developed to classify the corn kernels based on their colour, texture, and shape features. To accomplish an accurate classification, a line profile segmentation algorithm is developed to separate the touching corn kernels.

2. Line Profile Segmentation Algorithm

2.1. Hypothesis

The hypotheses of developing the novel segmentation algorithm are: (1) the corn has an elliptical shape, (2) the touching between the corn kernels is one dimensional by using a separator to arrange the corn in a form of single lines of touching corn, and (3) due to the elliptical shape of the corn, every two touching corn kernels will have a concavity between them.

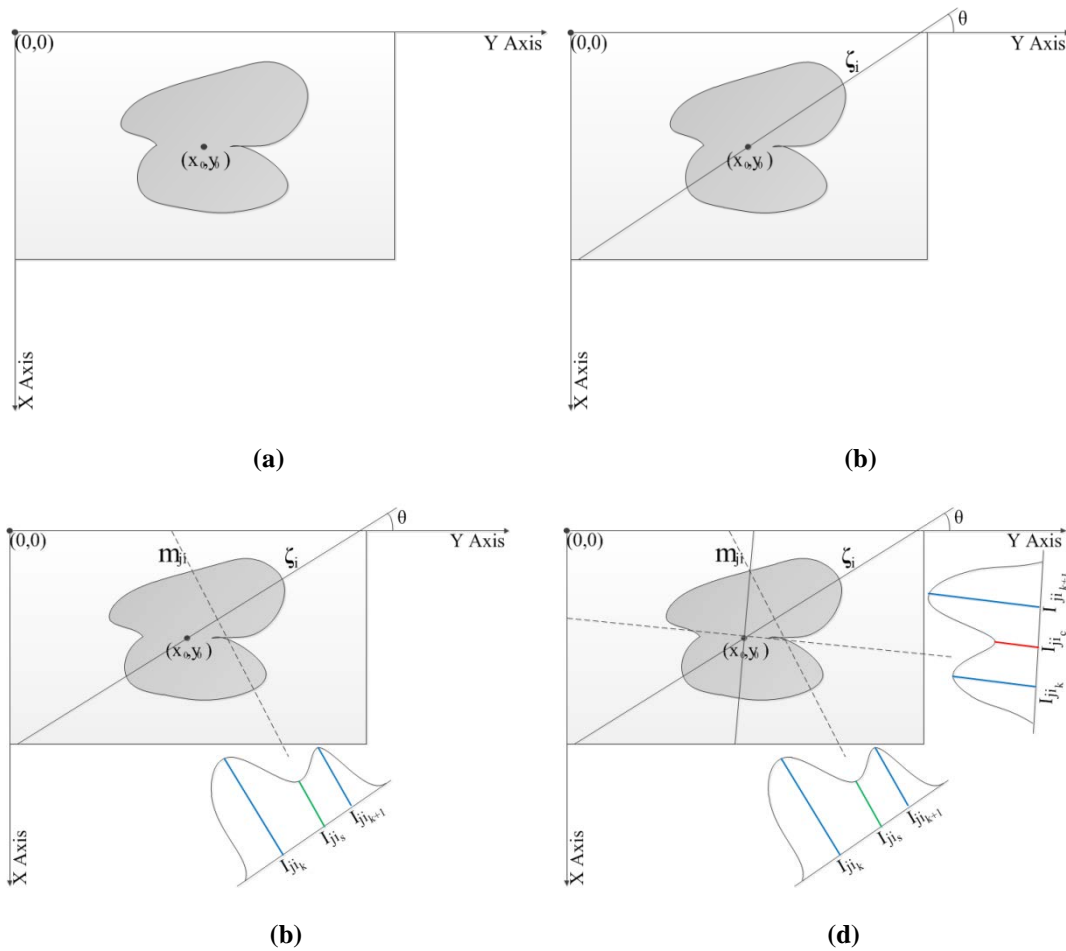


Figure 1. Illustrates (a) the coordinates of the touching corn image, (b) the base line rotated with a θ angle, (c) the profile created from the perpendicular lines, and (d) a comparison between different profiles.

2.2. Image Axis Line and Perpendicular Line

An RGB image(A) is converted to binary (B) using Otsu's method ^{20, 21}, to separate objects from

the background. The black background in the binary image represents the illumination brightness in the RGB image, while the white objects are corn kernels, and marking 0 being black, 1 being white. Objects are extracted to individual images. An object image can be an isolated corn kernel or a group of two or more touching corns. In an object image, the centroid is determined, and axis line points are determined using the following equation:

$$\zeta_j = \{ (x, y) | y = y_c + t \cos(\theta_j), x = x_c + t \sin(\theta_j), t \in (-\infty, +\infty) \} \quad (1)$$

where ζ_j is the axis line when angle is θ_j , (x, y) is coordinates of any point on the axis line, (x_c, y_c) is the coordinates of centroid, t determines points on the axis line located inside the object image, and θ_j is the angle of the axis line where if $j=1$ then the angle is the initial state, where $\theta_1=0$ (as shown in Figures 1(a) and 1(b)).

Points are selected on the axis line to be centroids for drawing perpendicular lines²². The distance (τ) is a constant, and represents the distance of adjacent perpendicular line in the axis line. Perpendicular lines are created using the following equation:

$$m_{ji} = \{ (s, t) | t = y(i) + h \cos\left(\frac{\pi}{2} - \theta_j\right), s = x(i) + h \sin\left(\frac{\pi}{2} - \theta_j\right), h \in (-\infty, +\infty) \} \quad (2)$$

where m_{ji} is a perpendicular line and represents the 'i'th perpendicular line on the 'j'th axis line, (s, t) is coordinates of any point on the perpendicular line, and h is the distance between the points in the perpendicular line (as shown in Figure 1(c)).

2.3. Definition of Profile

The summation of pixel values along the perpendicular line (m_{ji}) is calculated as follow:

$$I_{ji} = \arg \int_{ij} m_{ji} dm \quad (3)$$

where I_{ji} is the sum of pixel values across the perpendicular line (m_{ji}). A profile is a set, and the set is comprised with the sum of pixel values of all perpendicular lines in an axis line inside the object image. Resolution of a profile is scaled by distance (τ).

$$p = \{ I_{j1}, I_{j2}, \dots, I_{ji}, \dots, I_{jn} \} \quad (4)$$

where p is a profile, n represents the maximum number which contains perpendicular line inside the object image.

2.4. Establishment of Split Line

Since corn has an elliptical shape, a profile of an object can be a single nodule for isolated corn kernels or multi-nodule for two or more touching corns. A single profile cannot determine if the object is a single corn or multitude of corn kernels. Therefore, a series of profiles from different angles are obtained for an object image. The number of nodules is determined by calculating the highest peak for every nodule in the profile. Concavities between the peaks indicate concavities between the touching corns. Threshold μ determines if the concavity in the profile is possibly a concavity between the touching corn kernels in the object image. If the concavity point in the profile is equal or higher than the μ threshold, then the concavity can be selected as a possible split path. Searching for concavities is performed using the following equation:

$$I_{jik} - I_{jis} \geq \mu \ \& \ I_{jik+1} - I_{jis} \geq \mu \quad (5)$$

where I_{jik} is a peak point in the profile, and k is the location of the peak point in the profile. I_{jis} is the minimum point between the two peaks, and s is the location of the minimum point between every two peaks. If the minimum point I_{jis} satisfies the previous condition, then the minimum point is saved in a vector (ψ) to be compared to other concavity points obtained from all other profiles.

The first profile obtained is at angle $\theta_j=0$. To determine more profile the angle increases using the following equation:

$$\theta_j = j \times \delta, \text{ Where, } 0^\circ \leq \delta \leq 179^\circ \quad (6)$$

where δ is the amount of increment in the angle.

When a new angle is calculated, a new axis line and line profiles are generated. Therefore, a new profile is obtained. Generation of profiles will stop when θ is equal to 179° . The minimum value of all the concavity points saved in the vector(ψ) is determined as the following equation:

$$\xi = \arg \min (\psi) \quad (7)$$

where ξ is the minimum point that represents the concavity in the object image between the touching corns, where a split line is created using angle and point location on the axis line information (as shown in Figure1).

2.5. Line Profile Segmentation Algorithm

The algorithm proposed in this work combined several image processing techniques. Before using line profile segmentation, image was firstly converted to binary by Otsu's method, then calculated centroid of an object image by Matlab (shown in Figure 1a).

On the base of the above, the algorithm can be finished by the following procedure:

- Step 1: Optimize parameters τ and δ ;
- Step 2: According to equation (1), draw an axis line (as shown in Figure 1b);
- Step 3: According to equation (2) and parameter τ , draw perpendicular line on an axis line (as shown in Figure 1c);
- Step 4: According to equation (3) and equation (4), calculate the sum of pixel values across the perpendicular line and construct profile;
- Step 5: Establish a curve by a set of profiles on an axis line (as shown in Figure 1d);
- Step 6: According to equation (5), save concavity point (I_{jis}) in the curve into vector (ψ);
- Step 7: According to equation (7), get the minimum point in the object image from vector (ψ), that is the concavity in the object image between the touching corns.

2.6. Processing of segmentation using the method

Objects of the image are extracted to individual images. In every individual image a set of profiles is determined. These profiles indicate if the object in the object image is an isolated corn kernel or a group of touching corns using line profile segmentation. If the profiles of an object are uni-nodule profiles, then a flag value is set to zero to indicate this object is an isolated corn and the corn kernel is saved as an image. If any or some of the profiles of an object are multi-nodules profiles, then the flag is set to one to indicate that the object is a two or more touching corn, and line profile algorithm will repeat on the same object until all corns are separated from in that object image and the flag becomes zero (as shown in Figure 2).

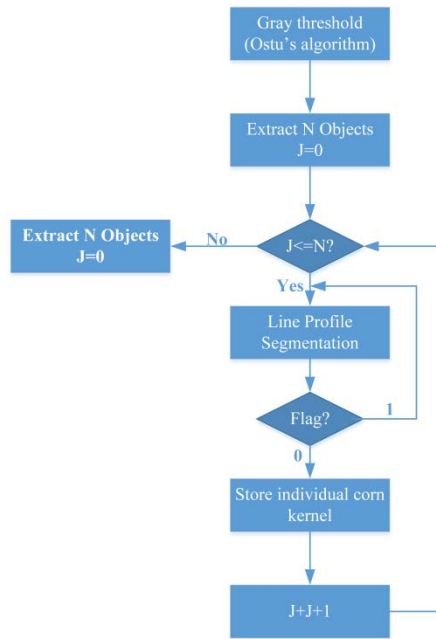


Figure 2. The segmentation process is explained by a flow chart

3. Experimental Design and Results

3.1. Experimental Method and Tool

This paper simultaneously adopts line profile (LP) and watershed (WS) segmentation algorithms to the same experimental materials and conditions. All the experimental images are acquired by a DFK 72BUC02 colour CMOS camera (2592×1944) with M12VM412 lens, the algorithms are implemented by Matlab.

3.2. Experimental Material

Three data sets of images were captured to verify and evaluate performance of the line profile segmentation. The first dataset is isolated corn (IC), where all the corns are separated from each other. The second dataset is designed pattern (DP), where corns are arranged in lines. The third dataset is random distributed (RD), in which the corns are randomly distributed on the imaging plate (Figure 3). Table 1 summarizes the description of the experimental data sets. The corns were placed on the imaging table in area of 10 inch × 8 inch. Nine designed pattern images and twenty random distributed images were captured and saved in a BMP format. A LP algorithm was developed, and a WS segmentation method was downloaded from the Internet. The two algorithms will be applied to each image in the datasets and segmentation result will be

evaluated and compared.

Table 1. Experimental conditions

Pattern	Description
Isolated Corn (IC)	All the corn are separated from each other
Designed Pattern (DP)	Corn arranged in separated lines. Each line is a single stripe of touching corn.
Random Distributed (RD)	Corn dumped randomly on the imaging plate.

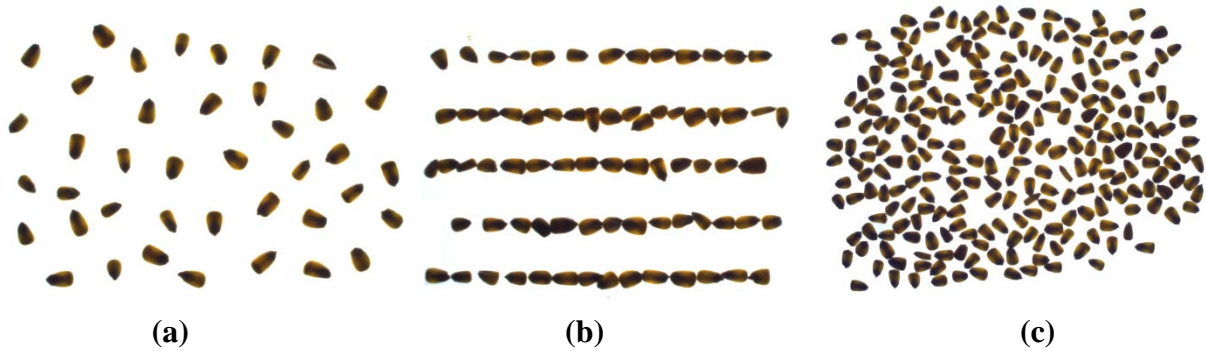


Figure 3: Illustrates (a) Isolated corn pattern, (b) single line formation, and (c) random distributed pattern.

3.3. Parameters Optimization of LP Algorithm

For the optimization of LP algorithm, the designed pattern (DP) of images is applied to verify the three optimal thresholds. To validate the performance of the LP algorithm, the result of segmentation was compared to the results of WS method by using the isolated corn (IC), designed pattern (DP) and random distributed (RD).

The result of the segmentation of both patterns is recorded. The recorded results are the actual number of the corn, segmentation time in seconds, correct segments, missed segments or un-segmented corn, over-segmented, wrong segments (missed segments and over segmentation) and segmentation rate. The segmentation rate is a percentage of the number of correct segments to the total number of the corn.

$$S_r = \frac{C_s}{N} \times 100 \quad (8)$$

where, S_r is the segmentation rate, C_s is the number of correct segments, and N is the actual number of corn in the image.

3.3.1 Optimization steps

Two steps are applied to optimize the parameters of LP algorithm. The first step is to optimize the distance between two points on the axis line is a threshold (τ) to decide the distance between the perpendicular lines. The second optimization concerns finding the ultimate angle increment (δ). Both steps compare three different values of the threshold for accepting concavities (μ) at 5%, 15%, and 25% of the average length of the corn. Table 2 shows the optimization results for step 1, and Table 3 shows the optimization results for step 2.

Table 2. Optimization of the distance (τ) at angle increment of 1°

	Correct seg.	Wrong Seg.	Seg. Rate (%)	Seg. Time (sec)
a) $\tau = 1$:				
$\mu = 5\%$	67.6 \pm 2.1	1 \pm 1.7	99.2 \pm 1.5	1517.9 \pm 986.4
$\mu = 15\%$	68.1 \pm 2.2	0 \pm 0	100 \pm 0	1476 \pm 984.9
$\mu = 25\%$	68.1 \pm 2.2	0 \pm 0	100 \pm 0	1502.9 \pm 966.4
b) $\tau = 3$:				
$\mu = 5\%$	67.3 \pm 2.4	1.3 \pm 1.8	98.9 \pm 1.8	520.8 \pm 338.9
$\mu = 15\%$	68.1 \pm 2.2	0 \pm 0	100 \pm 0	507.1 \pm 319.1
$\mu = 25\%$	68.1 \pm 2.2	0 \pm 0	100 \pm 0	497.3 \pm 315.2
c) $\tau = 5$:				
$\mu = 5\%$	67.6 \pm 2.7	0.8 \pm 1.7	99.2 \pm 1.7	301.3 \pm 187.5
$\mu = 15\%$	68.1 \pm 2.2	0 \pm 0	100 \pm 0	306.1 \pm 193.8
$\mu = 25\%$	67.9 \pm 2.6	0 \pm 0	99.7 \pm 1	302.3 \pm 189.4
d) $\tau = 7$:				
$\mu = 5\%$	67.9 \pm 2.2	0.3 \pm 1	99.7 \pm 1	215.4 \pm 134.8
$\mu = 15\%$	68.1 \pm 2.2	0 \pm 0	100 \pm 0	221.3 \pm 139.8
$\mu = 25\%$	67.9 \pm 2.6	0.1 \pm 0.3	99.7 \pm 1	222.6 \pm 139.7
e) $\tau = 9$:				
$\mu = 5\%$	65.2 \pm 3.4	3 \pm 2.9	95.8 \pm 3.9	171.8 \pm 104.3
$\mu = 15\%$	66.1 \pm 3.3	1.7 \pm 2.4	97.1 \pm 3.9	171.9 \pm 107.6
$\mu = 25\%$	64.8 \pm 3.5	1.9 \pm 1.5	95.1 \pm 3.3	169.2 \pm 105.6
f) $\tau = 11$:				
$\mu = 5\%$	56.3 \pm 6.8	9.4 \pm 6.1	82.8 \pm 10.7	138.8 \pm 87.7
$\mu = 15\%$	57.2 \pm 6.4	7.4 \pm 4.7	86.8 \pm 9.7	141 \pm 90.4
$\mu = 25\%$	53.7 \pm 7.4	7.9 \pm 4.5	78.9 \pm 11.3	133.7 \pm 86.9
g) $\tau = 13$:				
$\mu = 5\%$	47.2 \pm 9.1	13.9 \pm 6.7	69.5 \pm 13.5	112.2 \pm 73.3
$\mu = 15\%$	46.1 \pm 9.2	13.4 \pm 6.3	61.8 \pm 24.1	110.1 \pm 73.5
$\mu = 25\%$	42.3 \pm 10.3	13.9 \pm 5.6	62.3 \pm 15.4	105.6 \pm 74.5
h) $\tau = 15$:				
$\mu = 5\%$	32 \pm 5.5	20.8 \pm 3.4	47 \pm 8.2	80.9 \pm 54
$\mu = 15\%$	31.9 \pm 6.7	19.8 \pm 3.6	46.8 \pm 10	81.9 \pm 55.8
$\mu = 25\%$	29 \pm 5.4	20.2 \pm 2.6	42.6 \pm 8.4	76.4 \pm 53.6

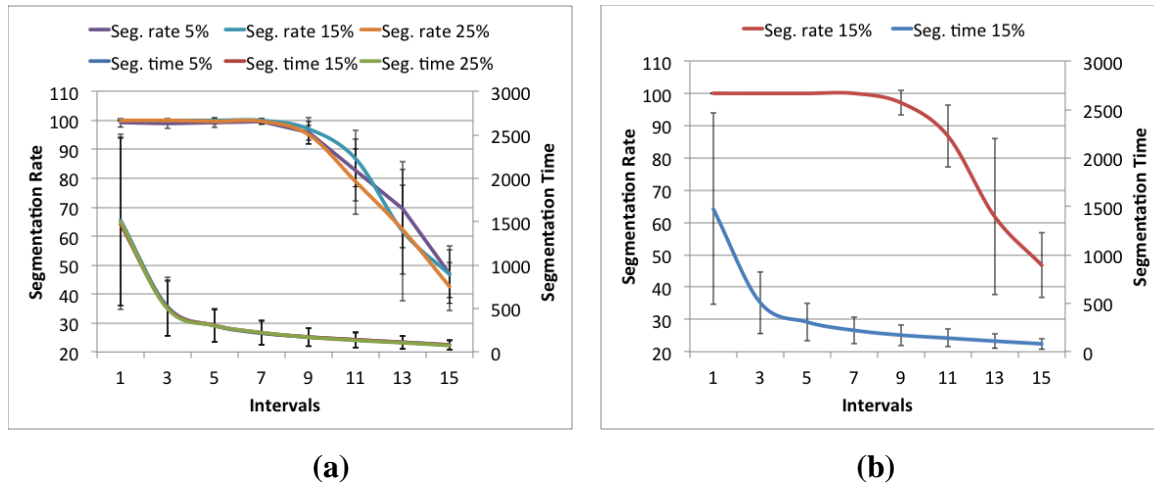


Figure 4: (a) Segmentation time and rate of three values of μ at different intervals (b) segmentation time and rate of $\mu = 15\%$.

3.3.2. Optimization of parameter τ

In step 1, the segmentation results using the threshold for accepting concavities (μ) shows close results in both segmentation time and segmentation rate during different distance range as shown in Figure 4a. From Figure 4b, when the accepting concavities threshold (μ) equals to 15% of the average length of the corn, the segmentation rate starts dropping when the distance (τ) between points on the axis line is larger than 7 and drops significantly when τ equals to 11. The segmentation time drops from distance threshold (τ) of 1 to 5 significantly then from distance threshold (τ) of 5 the segmentation time drop slightly with no significant difference. Running results is shown in Table 2.

3.3.3. Optimization of parameter δ

In step 2, Figure 5a shows that the segmentation results using the threshold for accepting concavities (μ) at 5%, 15%, and 25% of the average length of the corn shows no significant difference. Figure 5b shows the segmentation results using μ equal to 15% of the average length of the corn. The segmentation rate show steady performance at 100% segmentation rate from degree threshold (δ) equals to 1 until 9 degree, then drops slightly from (δ) of 12 degree, and then drops significantly from (δ) of 20 degrees comparing to 9 degree. The segmentation time drops significantly from (δ) of 1 degree to 5 degree. After 5 degree the time drops slightly. Running results is shown in Table 3.

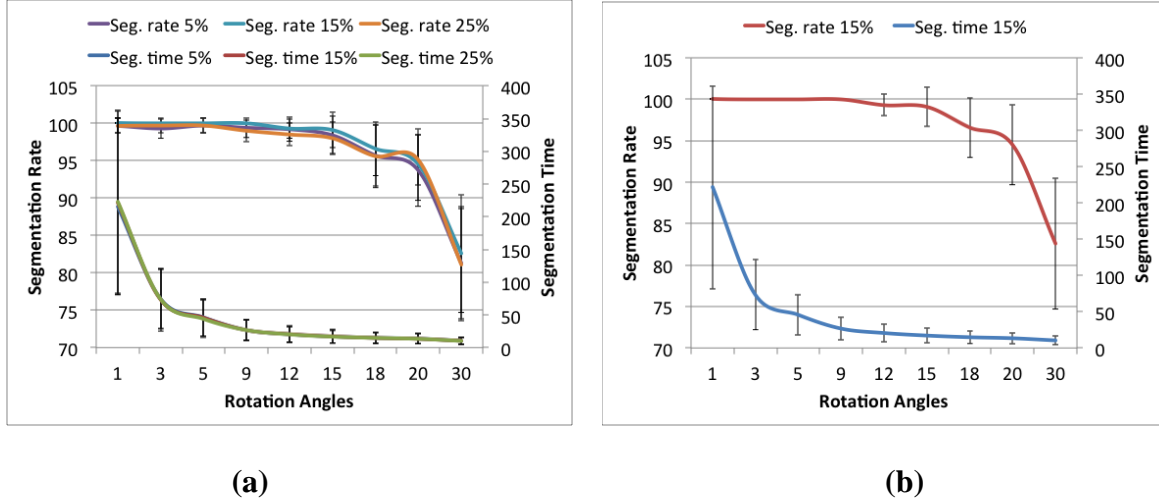


Figure 5: (a) Segmentation time and rate of three values of μ at different angles (b) segmentation time and rate of $\mu = 15\%$.

Table 3. Optimization of the angle increment (δ) at 7 points distance between points on the axis line.

	Correct seg.	Wrong Seg.	Seg. Rate (%)	Se. Time (sec)
a) $\delta=1$:				
$\mu = 5\%$	67.9 \pm 2.2	0.3 \pm 1	99.7 \pm 1	215.4 \pm 134.8
$\mu = 15\%$	68.1 \pm 2.2	0 \pm 0	100 \pm 0	221.3 \pm 139.8
$\mu = 25\%$	67.9 \pm 2.6	0.1 \pm 0.3	99.7 \pm 1	222.6 \pm 139.7
b) $\delta=3$:				
$\mu = 5\%$	67.7 \pm 2.6	0.6 \pm 1.1	99.3 \pm 1.3	74.4 \pm 45.7
$\mu = 15\%$	68.1 \pm 2.2	0 \pm 0	100 \pm 0	73.3 \pm 48.1
$\mu = 25\%$	67.9 \pm 2.6	0.1 \pm 0.3	99.7 \pm 1	73.9 \pm 45.4
c) $\delta=5$:				
$\mu = 5\%$	67.9 \pm 2.2	0.3 \pm 1	99.7 \pm 1	46.2 \pm 28.5
$\mu = 15\%$	68.1 \pm 2.2	0 \pm 0	100 \pm 0	45.7 \pm 28.3
$\mu = 25\%$	67.9 \pm 2.6	0.1 \pm 0.3	99.7 \pm 1	43.8 \pm 28.7
d) $\delta=9$:				
$\mu = 5\%$	67.7 \pm 2.1	0.7 \pm 1.3	99.4 \pm 1.3	26.7 \pm 15.6
$\mu = 15\%$	68.1 \pm 2.2	0 \pm 0	100 \pm 0	26.7 \pm 15.8
$\mu = 25\%$	67.4 \pm 2.8	0.3 \pm 0.5	99 \pm 1.5	26.7 \pm 15.8
e) $\delta=12$:				
$\mu = 5\%$	67.6 \pm 2.3	0.7 \pm 1.4	99.2 \pm 1.6	20.4 \pm 12.2
$\mu = 15\%$	67.7 \pm 2.3	0.4 \pm 0.9	99.3 \pm 1.3	20.1 \pm 12.4
$\mu = 25\%$	67.1 \pm 2.1	0.7 \pm 0.7	98.5 \pm 1.5	20.2 \pm 12.2
f) $\delta=15$:				
$\mu = 5\%$	67 \pm 2.4	1.2 \pm 2	98.4 \pm 2.5	17 \pm 9.9
$\mu = 15\%$	67.4 \pm 2.2	0.7 \pm 1.7	99.1 \pm 2.4	17.1 \pm 10.1
$\mu = 25\%$	66.8 \pm 2.6	0.8 \pm 0.8	98 \pm 2.2	16.9 \pm 10
g) $\delta=18$:				
$\mu = 5\%$	65.1 \pm 2.8	3.1 \pm 3.1	95.7 \pm 4.1	14.9 \pm 8.6
$\mu = 15\%$	65.8 \pm 2.4	2.3 \pm 2.5	96.6 \pm 3.6	14.8 \pm 8.7
$\mu = 25\%$	65.1 \pm 3.1	2.3 \pm 02.5	95.6 \pm 4.2	14.8 \pm 8.7
h) $\delta=20$:				
$\mu = 5\%$	63.8 \pm 2.6	4.3 \pm 3.4	93.7 \pm 4.8	13.6 \pm 7.6

$\mu = 15\%$	64.3 ± 3.2	3.8 ± 3.3	94.5 ± 4.8	13.4 ± 7.7
$\mu = 25\%$	64.8 ± 2.4	2.6 ± 1.7	95.1 ± 3.4	13.4 ± 7.7
i) $\delta=30$:				
$\mu = 5\%$	55.3 ± 4.7	13.3 ± 5.3	81.3 ± 7.5	10.4 ± 5.8
$\mu = 15\%$	56.2 ± 5.2	11.9 ± 5.5	82.6 ± 7.9	10.4 ± 5.8
$\mu = 25\%$	55.2 ± 4.8	10.2 ± 4.2	81.1 ± 7.5	10.2 ± 5.6

3.4. Comparison Between LP and WS Algorithms

Line profile segmentation (LP) and watershed (WS) were applied to three patterns of images to compare the segmentation results. The patterns are: isolated corn (IC), designed pattern (DP), and random distributed corn (RD). The line profile thresholds applied are: μ equals to 15% of the average length of the corn, distance threshold (τ) equals to 7, and angle increment degree (δ) equals to 9° . The segmentation results are illustrated in table 4. Figure 6 shows a comparison between line profile and watershed method in segmentation rate and segmentation time.

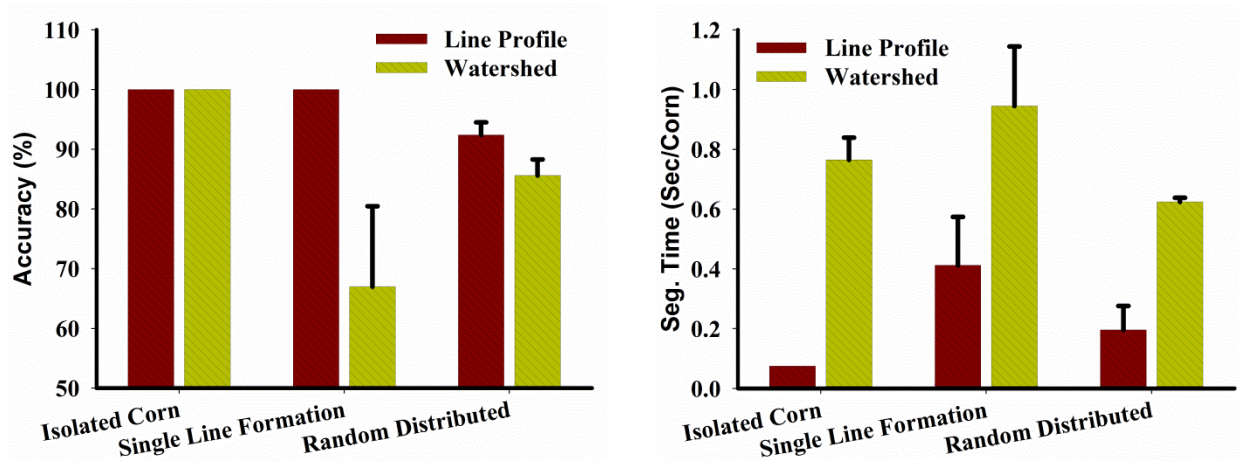


Figure 6. Comparison between WS and LP segmentation using three patterns of images. The comparison is for (left) segmentation rate, and (right) segmentation time.

When both algorithms are applied to IC pattern, both algorithms successfully separate all the corn from the background of the image, as shown in Figures 7a and 7b. Anyhow, the segmentation time for LP is significantly lower than the segmentation time of WS, where the segmentation time is 3 ± 0.1 and 30.5 ± 2.9 for LP and WS, respectively.

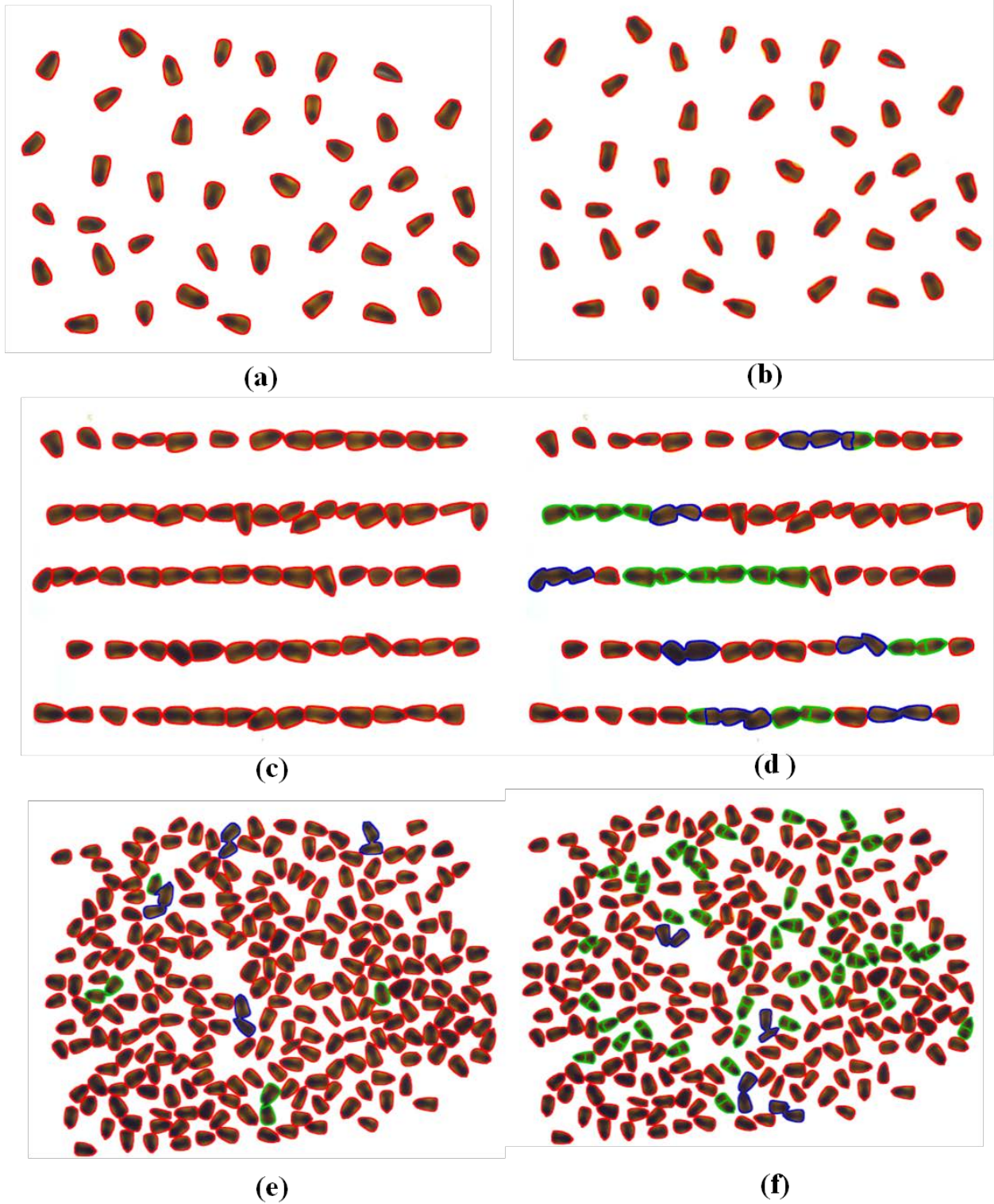


Figure 7. Illustrates in colors the segmentation results of: (a) LP segmentation of IC pattern, (b) WS segmentation of IC pattern, (c) LP segmentation of DP pattern, (d) WS segmentation of DP pattern, (e) LP segmentation of RD pattern, and (f) WS segmentation of RD pattern

The LP segmentation successfully separates all the corn when it is applied to DP pattern and significantly higher than the segmentation rate of the watershed (WS) applied to the same pattern. Where the segmentation rate of LP is 100% and the segmentation rate of WS is $66.97\% \pm 13.5$. Figure 7c shows that LP separates all the corn correctly, while Figure 7d illustrates that WS caused missed segments, and over segmentation. LP segmentation time is significantly lower than WS segmentation time. LP consumes 31.1 ± 12.7 seconds, while WS consumes 45 ± 3.3 .

Table 4. Comparison between the segmentation results of LPS and WS.

	Num. of Corn	Correct Seg.	Missed Seg.	Over Seg.	Seg. Rate (%)	Time (sec)
a) Isolated corn:						
Line Profile	40 ± 0	40 ± 0	0 ± 0	0 ± 0	100 ± 0	3 ± 0.1
Watershed	40 ± 0	40 ± 0	0 ± 0	0 ± 0	100 ± 0	30.5 ± 2.9
b) Single lines formation:						
Line Profile	73.9 ± 6.3	73.9 ± 6.3	0 ± 0	0 ± 0	100 ± 0	31.1 ± 12.7
Watershed	73.9 ± 6.3	49.5 ± 10.8	6.6 ± 2.7	9.7 ± 5.1	66.97 ± 13.5	45 ± 3.3
c) Random Distributed:						
Line Profile	250 ± 0	231 ± 5.3	4.4 ± 2	10.4 ± 5.5	92.4 ± 2.1	49.1 ± 20.1
Watershed	250 ± 0	214.1 ± 6.7	2.4 ± 1.6	58.4 ± 9	85.6 ± 2.7	156 ± 5.6

At the RD pattern of corn, LP segmentation rate equals to $92.4\% \pm 2.1$ is still significantly higher than the segmentation rate of WS at $85\% \pm 2.7$. Figure 7e shows that even though LP caused missed segments and over segmentation, but separated most of the corn correctly. Figure 7f shows that WS have caused multiple missed segments, and many over segmentation. The segmentation time of LP is significantly lower than WS, where the segmentation time of LP is 49.1 ± 20.1 seconds, and 156 ± 5.6 for WS.

4. Conclusions

A novel image segmentation algorithm is developed for splitting touching corn kernels based on profiles and concavities. It includes optimizing parameters, constructing profiles, seeking concavity points and getting a splitting path. The experimental results show that it provides a fast and accurate segmentation method for splitting touching corn kernels. Because the algorithm is faster and more accurate segmentation method, it is used to grains qualify classification on agricultural production. Meantime, it can be applicable not only to images of clustered corn kernels, but also to images of other particles in different sizes and shapes under hypothesis that

objects are convex or nearly convex, e.g. rice kernels, soybean, and other similar crops images.

In the next research, we will improve efficiency and accuracy of the algorithm for service of agricultural production through improving image compression rate and reducing the amplitude of profiles.

5. References

1. USDA, "World Agricultural Supply and Demand Estimates", 2017.
2. USDA, (United States Department of Agriculture, 2013).
3. Y. Qin, W. Wang, W. Liu and N. Yuan, "Extended-Maxima Transform Watershed Segmentation Algorithm for Touching Corn Kernels", *Advances in Mechanical Engineering*, (2013).
4. B. Ni, M. Paulsen and J. Reid, "Size Grading of Corn Kernels with Machine Vision", *Applied Engineering in Agriculture*, **14**(567-571), (1998).
5. L. Steenoek, M. K. Misra, C. Hurburgh and C. J. Bern, "Implementing a Computer Vision System for Corn Kernel Damage Evaluation", *Applied Engineering in Agriculture*, **17**(2), 235-240, (2001).
6. X. Chen, Y. Xun, W. Li and J. Zhang, "Combining Discriminant Analysis and Neural Networks for Corn Variety Identification", *Computers and electronics in agriculture*, **71**(S48-S53), (2010).
7. J. Qin and L. Xu, "Engineering Modelling of Data Acquisition and Digital Instrumentation for Intelligent Learning and Recognition", *Biosens J*, **4**(1), 103, (2015).
8. J. Qin, P. Sun and J. Walker, "A Waveform Profile-Based Noise Measurement System and Methodology for Complex Noise Evaluation", *Noise Control Engineering Journal*, **63**(6), 563-571, (2015).
9. A. Mahdi, M. Su, M. Schlesinger and J. Qin, "A Comparison Study of Saliency Models for Fixation Prediction on Infants and Adults", *IEEE Transactions on Cognitive and Developmental Systems*, (2017).
10. J. Qin and P. Sun, "Applications and Comparison of Continuous Wavelet Transforms on Analysis of a-Wave Impulse Noise", *Archives of Acoustics*, **40**(4), 503-512, (2015).
11. J. Qin, "Numerical Analysis of Bubble Dynamics in Electrohydraulic and Electromagnetic Shock Wave Lithotripsy", *International Journal of Computational Biology and Drug Design*, **8**(2), 105-113, (2015).
12. Q. Wu and J. Qin, "Effects of Key Parameters of Impulse Noise on Prediction of the Auditory Hazard Using Ahaah Model", *International journal of computational biology and drug design*, **6**(3), 210-220, (2013).
13. B. Ni, M. Paulsen and J. Reid, "Corn Kernel Crown Shape Identification Using Image Processing", *Transactions of the ASAE-American Society of Agricultural Engineers*, **40**(3), 833-838, (1997).
14. J. M. Valiente-González, G. Andreu-García, P. Potter and Á. Rodas-Jordá, "Automatic Corn (Zea Mays) Kernel Inspection System Using Novelty Detection Based on Principal Component Analysis", *biosystems engineering*, **117**(94-103), (2014).

15. D. Jayas, J. Paliwal and N. Visen, "Review Paper (Ae—Automation and Emerging Technologies): Multi-Layer Neural Networks for Image Analysis of Agricultural Products", *Journal of Agricultural Engineering Research*, **77**(2), 119-128, (2000).
16. W. Wang and J. Paliwal, "Separation and Identification of Touching Kernels and Dockage Components in Digital Images", *Canadian biosystems engineering*, **48**(7), (2006).
17. M. Faessel and F. Courtois, "Touching Grain Kernels Separation by Gap-Filling", *Image Analysis & Stereology*, **28**(3), 195-203, (2011).
18. Q. Zhong, P. Zhou, Q. Yao and K. Mao, "A Novel Segmentation Algorithm for Clustered Slender-Particles", *Computers and Electronics in Agriculture*, **69**(2), 118-127, (2009).
19. L. Yan, C.-W. Park, S.-R. Lee and C.-Y. Lee, "New Separation Algorithm for Touching Grain Kernels Based on Contour Segments and Ellipse Fitting", *Journal of Zhejiang University-Science C*, **12**(1), 54-61, (2011).
20. R. C. Gonzalez and R. E. Woods, *Digital Imaging Processing*, (2008).
21. N. A. Malalla, P. Sun, Y. Chen, M. E. Lipkin, G. M. Preminger and J. Qin, "C-Arm Technique with Distance Driven for Nephrolithiasis and Kidney Stones Detection: Preliminary Study", *Biomedical and Health Informatics (BHI), 2016 IEEE-EMBS International Conference on*, 164-167, (2016).
22. J. Qin, "Computational Analysis and Monte Carlo Simulation of Wave Propagation", *International Journal of Computational Biology and Drug Design*, **8**(2), 159-167, (2015).